Diffractive phase element for reducing a diameter of main-lobe of a focal spot

Yusuke Ogura[a], Jun Tanida[a], Yoshiki Ichioka[b], Yoshiaki Mokuno[c], and Katsunori Matsuoka[c]

[a]Graduate School of Engineering, Osaka University,
2-1 Yamadaoka, Suita, Osaka, 565-0871 Japan
[b]Nara National College of Technology,
22 Yata-cho, Yamatokoriyama, Nara, 639-1080 Japan
[c]Department of Optical Materials, Osaka National Research Institute,
1-8-31 Midorigaoka, Ikeda, Osaka, 563-8577 Japan

ABSTRACT

A diffractive phase element (DPE) reducing the diameter of main-lobe of a focal light spot has been developed. A light spot focused by an optical system spreads due to the light diffraction from a limited aperture of lens. The developed DPE reduces the main-lobe diameter by modulating the incident wave-front of the focusing lens. Although the DPE increases the side-lobe intensity of the focal spot, appropriate design can reduce its magnitude enough not to affect the photoresist in lithography process. An iterative method based on the Gerchberg-Saxton algorithm combined with new constraints was applied to design a DPE. A rotation symmetrical binary DPE was designed, which reduces the main-lobe diameter to 74% and makes the side-lobe intensity under 2.7% of the main-lobe. The designed DPE was fabricated with the laser beam lithography system developed by the authors, and its performance was measured by mounting it on this system. The minimum line width obtained with the DPE becomes 1.0μm while it is 1.2μm without the DPE. It is also shown by a computer simulation that the focal depth of the focusing system with the DPE becomes wider than that without the DPE when both systems produce the same focal spot size.

Keywords: diffractive phase element, focusing system, focal depth, focal spot pattern, laser beam lithography

1. INTRODUCTION

Diffractive phase elements (DPEs) have considerably extended their applications according as the development of microfabrication technology, which enables us to realize various optical functions, an optical integration of numerous optical systems, or a easy replication for optical elements. Especially, DPEs have ability to create distinctive optical functions designed by a computer with high efficiency of light usage in a thin element. So DPEs have been applied as special optical elements such as optical interconnections,[1] beam shaping,[2] mode formers[3] and so on.

In order to obtain the desired functions of a DPE, it is important to design a proper surface relief of a element. The Simulated Annealing method (SA)[4] and an iterative method based on the Gerchberg-Saxton algorithm (GSA)[5] are well-known methods for designing DPEs. The SA method can design DPEs with high accuracy, but needs heavy computational load than the GSA. On the other hand, the GSA leads a desirable answer in a short time but it needs a proper constraints to converge in many cases. For example, it was reported that the GSA produced the DPE in only 20 iterations, which converts a Gaussian beam profile to a uniform intensity distribution.[6]

DPEs are usually fabricated by using lithography and etching processes. The functions of DPEs are often restricted by a fabrication limit, that is, finer structures than the spot size determined by diffraction limit of the focusing lens can not be achieved. We attempt to make finer structures than the spot size determined by diffraction limit by using a DPE. The DPE, we used, is designed by the GSA with special constraints. It modulates a wave-front of the incident light to the focusing lens of a photolithography system as illustrated in Fig. 1, and generates a smaller spot size than diffraction limit but it allows a little increase of side-lobe intensity. This technique looks similar to an apodization technique, that is well-known to obtain wider focal depth in an imaging system.[7–9] But an apodization technique usually spreads a focal spot pattern for concentrating light energy of side-lobes to main-lobe. For our purpose, it is more important to make a light spot sharp than to concentrate light energy to main-lobe, even if a

Correspondence: E-mail: ogura@mls.eng.osaka-u.ac.jp

In *Optical Storage and Optical Information Processing*, Han-Ping D. Shieh, Tom D. Milster, Editors, Proceedings of SPIE Vol. 4081 (2000) • 0277-786X/00/$15.00

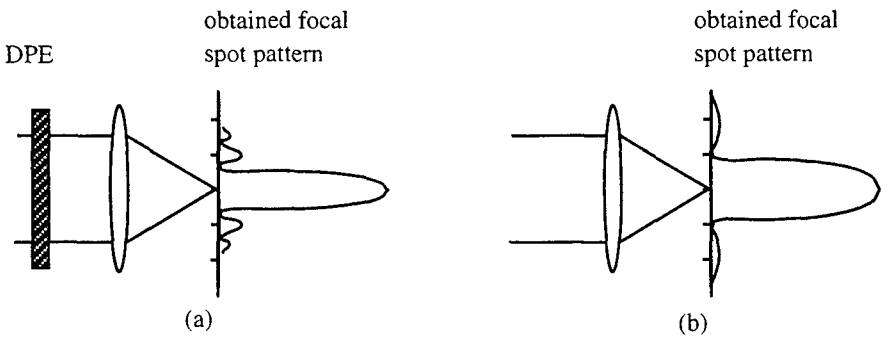

Figure 1. Scheme of a focusing system for reducing spot size; (a) with the DPE, and (b) without a DPE (a conventional system).

side-lobe intensity might increase. In the lithography process, an effect of the side-lobe intensity to pattern drawing can be eliminated because of the nonlinear sensitivity of a photoresist material.

In this paper, we describe the design method for the DPE, its implementation, and its evaluation by optical experiments. The DPE is designed by a modified GSA with new constraints. The designed DPE is fabricated by using the laser beam lithography system we developed, and it is mounted on the system for evaluation. The drawing resolution is evaluated from experimental results. We also discuss on the focal depth of the focusing system with or without the DPE, and performance of the DPE is evaluated.

2. DESIGN OF THE DPE

2.1. Design Method

Design of a DPE is performed by two steps. The first step is to calculate the continuous phase distribution of a DPE, and the second step is to quantize the calculated phase distribution. In this paper, the GSA is basically applied in the first step and the stepwise quantization method (SQM) proposed by Wyronski[10] is used in the second step. The design procedure for the GSA is described as the following six steps, in which l denotes the iteration number and an observation plane means a focal plane of a focusing lens:

1. An initial phase distribution ψ_0 of a wave-front on the observation plane is chosen at random.
2. The wave-front on the DPE plane is calculated by inverse Fourier transform of the wave-front $\sqrt{\overline{I}_l}e^{i\psi_l}$ on the observation plane, where $\sqrt{\overline{I}_l}$ denotes an ideal amplitude of wave-front on the observation plane. It is expressed as $A_l e^{i\phi_l} (= F^{-1}[\sqrt{\overline{I}_l}e^{i\psi_l}])$, where F^{-1} is an operator for the inverse Fourier transform. The details of the ideal amplitude $\sqrt{\overline{I}_l}$ at lth iteration are described in Sec. 2.2.
3. The amplitude A_l of the wave-front on the DPE plane is replaced with the amplitude W_0 of the illuminating light source. (This is the DPE plane constraint.) The phase ϕ_l is maintained to be unchanged.
4. The wave-front on the observation plane is calculated by Fourier transform of the wave-front $W_0 e^{i\phi_l}$ on the DPE plane. It is expressed as $\sqrt{I_l}e^{i\psi_l} (= F[W_0 e^{i\phi_l}])$, where F is an operator for the Fourier transform.
5. The calculated amplitude $\sqrt{I_l}$ of the wave-front on the observation plane is replaced with the $(l+1)$th ideal amplitude $\sqrt{\overline{I}_{l+1}}$. (This is the observation plane constraint.) The phase ψ_l is maintained.
6. If the iteration number reaches at the prescribed number or $I_{err} \leq 0.01$ is satisfied, the iteration is stopped. Here, I_{err} is determined as $\sqrt{\frac{\iint (I_0 - I_l)^2 \, dS}{\iint I_0^2 \, dS}}$ which is the root mean square error of I_l and I_0, where I_l and I_0 are an obtained intensity distribution and an ideal intensity distribution on the observation plane, individually. If the condition is not fulfilled, return to the step 2.

The phase distribution obtained by the above algorithm is quantized by the SQM in the second step. The procedure of SQM is same as that of GSA except for adding the quantization of the phase ϕ_l to the DPE plane constraint in step 3. The SQM leads a quantized phase distribution gradually by extending the quantization area as the iteration process proceeding.[10] In the design procedure for DPEs, we used the same parameters for SQM as described in Ref. 10; that is, Q=5, P=10, and $\epsilon^{(1)} = 0.3$, $\epsilon^{(2)} = 0.5$, $\epsilon^{(3)} = 0.6$, $\epsilon^{(4)} = 0.7$, $\epsilon^{(5)} = 0.75$, $\epsilon^{(6)} = 0.8$, $\epsilon^{(7)} = 0.85$, $\epsilon^{(8)} = 0.9$, $\epsilon^{(9)} = 0.95$, and $\epsilon^{(10)} = 1.0$, where Q is the number of iteration in each subdivided cycle in which the quantization area is fixed, P is the total number of subdivided iteration cycles, and $\epsilon^{(p)}$ indicates ratio of a quantization area to the total area in the pth subdivided iteration cycle.

In the case of design for DPEs to generate a rotation symmetrical focal spot pattern, it is convenient to use the one dimensional Hankel transform instead of the two dimensional Fourier transform. The complex-amplitude distribution $T_s(\rho)$ of the focal spot pattern is expressed as the Hankel transform of the transmittance distribution $t_s(r)$ of the DPE as follows.

$$T_s(\rho) = \frac{2\pi}{\lambda f} \int_0^\infty t_s(r) J_0 \left(\frac{2\pi}{\lambda f} \rho r \right) r \, dr, \tag{1}$$

where λ denotes a wavelength, f is a focal length of a focusing lens, r and ρ are radial coordinates in a DPE plane and a spot pattern plane, respectively, J_0 is the first kind zeroth order Bessel function. The inverse Hankel transform is expressed with the same mathematical expression of Eq. (1). In actual design, the discrete Hankel transform can be calculated by using the quasifast Hankel transform algorithm in a computer.[11]

2.2. Design of DPE for Generating a Small Light Spot

As a preparation before designing a DPE based on the procedure described in Sec. 2.1, the profile of an incident beam on to the DPE has to be measured. The intensity distribution $I_{\mathrm{inc}}(r)$ for a laser beam can be expressed with a gaussian profile by introducing a parameter w_s as follows,

$$I_{\mathrm{inc}}(r) \propto \exp\left(-\frac{r^2}{w_s^2} \right). \tag{2}$$

The beam profile in our system was measured experimentally by using the knife edge method, and we obtained $w_s = 1.47\mu$m. From this result, W_0 in design process 3 is set to $\sqrt{I_{\mathrm{inc}}(r)}$ with $w_s = 1.47$.

As the observation plane constraint in the design procedure, the rules of Eq. (3) which is based on an adaptive-additive algorithm[12] is utilized.

$$\bar{I}_{l+1}(\rho) = \begin{cases} \alpha I_0(\rho) + (1-\alpha) I_l(\rho) & (\rho \geq \frac{1}{2}\rho_{1/e^2}), \\ I_0(\rho) & (\rho < \frac{1}{2}\rho_{1/e^2}), \end{cases} \tag{3}$$

where $I_0(\rho)$ is a target spot intensity pattern, $I_l(\rho)$ is a spot intensity pattern calculated in lth iteration, $\bar{I}_{l+1}(\rho)$ is a constrained pattern, ρ is a radial variable, and ρ_{1/e^2} is the radius at which the intensity $I(\rho_{1/e^2})$ becomes $1/e^2 I(0)$, where $I(\rho)$ is the spot pattern obtained without the DPE. The parameter α in Eq. (3) controls the strength of constraints.

For the design of the DPE to reduce a spot diameter, a target intensity distribution I_0 was given by

$$I_0 = \begin{cases} 1 & (\rho < \frac{1}{2}\rho_{1/e^2}), \\ 0.003 & (\rho \geq \frac{1}{2}\rho_{1/e^2}), \end{cases} \tag{4}$$

and the parameter α in Eq. (3) is selected as follows:

$$\alpha = \begin{cases} 1 & (l \leq 50), \\ 0.02 \times l & (51 \leq l \leq 100), \\ 2 & (101 \leq l \leq 150). \end{cases} \tag{5}$$

The total iteration number is set to 100 for the first step and to 50 for the second step, sampling number in each plane is 4096 on a radial axis by using the Hankel transform, and the number of the phase levels of the DPE is 2. The design results are shown in Fig. 2. Figure 2(a) is the amplitude profile of the incident beam, (b) is the phase

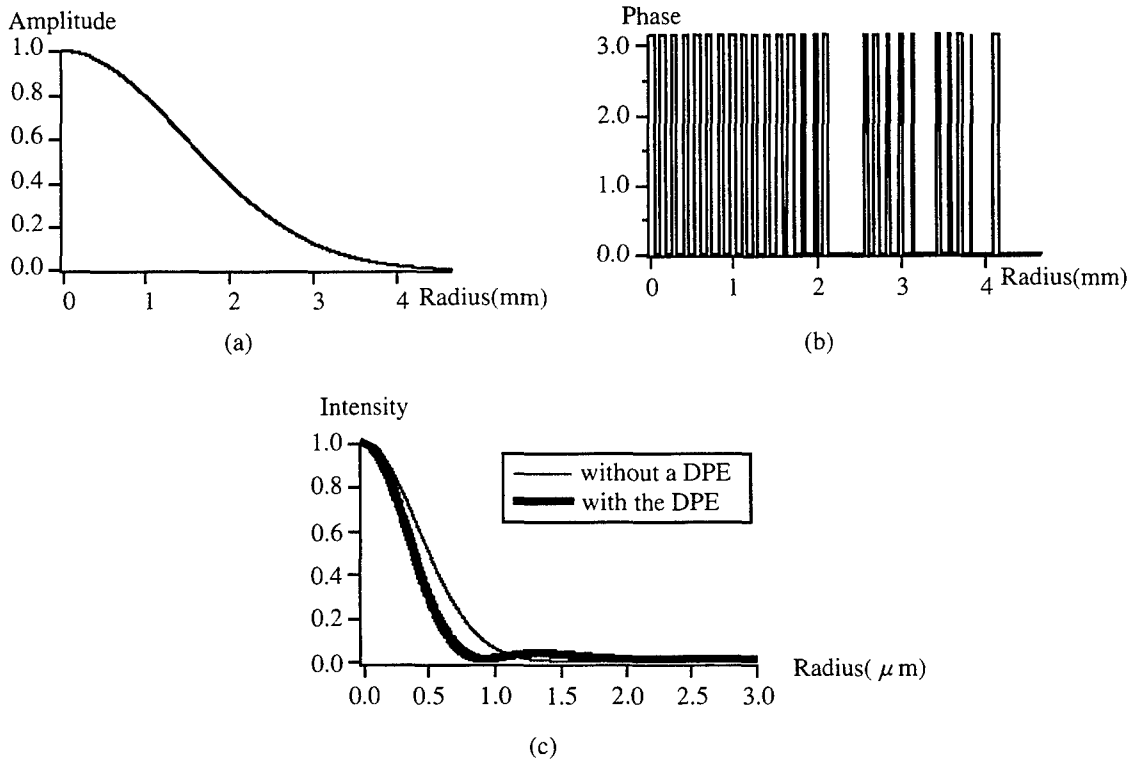

Figure 2. Design of the DPE; (a) amplitude profile of the incident beam, (b) phase distribution of the DPE, and (c) calculated focal spot pattern.

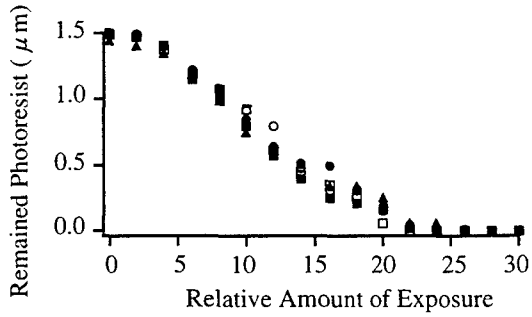

Figure 3. The relationship between the thickness of photoresist and exposure. Each marker denotes different measurements.

distribution of the designed DPE, and (c) is the calculated focal spot pattern obtained by using the designed DPE. The designed DPE reduces the spot radius from 0.85μm to 0.63μm, that is about 74% reduction, where we define a spot radius as a radius at which the spot intensity decreases to $1/e^2$ of main-lobe. On the contrary, the maximum side-lobe intensity increases to 2.7% of the main-lobe intensity. For an application of the laser beam lithography, side-lobe intensity should become small and not affect to the exposure. Figure 3 shows the relationship between the thickness of the remained photoresist after exposure and an amount of exposure, which we measured for the photoresist AZ1500 (Hoechst Industry Limited). This relationship shows that the side-lobe intensity less than 10% of the central intensity does not act on the exposure to the photoresist. Therefore, the DPE designed here can be utilized to improve the resolution of patterns drawn by a laser beam lithography system.

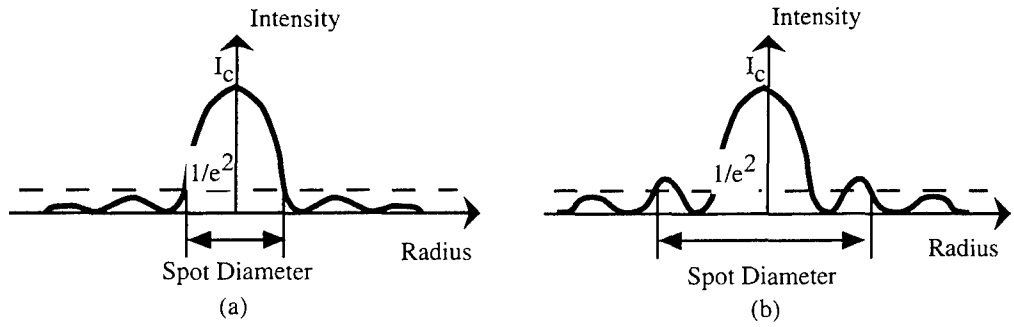

Figure 4. Definition of spot diameter. (a) Maximum side-lobe intensity is less than $1/e^2$ of main-lobe intensity and (b) more than $1/e^2$.

3. DISCUSSION ON FOCAL DEPTH OF FOCUSING SYSTEM WITH DPE

In a laser beam lithography process, a focused laser beam is scanned and exposes the photoresist coated on the glass substrate. The coated photoresist usually has thickness of sub micron meter or a few micron meter. So it is important not only to make a laser spot small but also to make the focal depth deep enough to obtain high resolution. In this section, we discuss on the focal depth of a focusing system with the DPE by comparing to other systems without the DPE.

3.1. Defocused Spot Pattern in a Focusing System

Let us consider a focusing system shown in Fig. 1(a). The spot pattern defocused by the amount of δd in the focusing system has the intensity distribution $I_\delta(\rho)$ of

$$I_\delta(\rho) \propto \left| \int t_s(r) \exp\left(ik\omega_{20} r^2\right) J_0\left(\frac{k}{f}\rho r\right) r\, dr \right|^2, \tag{6}$$

where $k = 2\pi/\lambda$, and

$$\omega_{20} = \frac{\delta d}{2}\mathrm{NA}^2, \tag{7}$$

in which NA is the numerical aperture of the optical system.[7,9] The other variables have same meanings as in Eq. (1).

Now we evaluate the focal depth for the three focusing systems as follows;

(i) Using a objective lens of NA=0.46 alone,

(ii) Using a objective lens of NA=0.46 with the DPE designed in Sec. 2.2,

(iii) Using a objective lens of NA=0.58 alone.

The number of NA in case (iii) is selected to get a same focal spot diameter as in case (ii). Now we define a spot diameter and a defocus distance for the following discussion. A spot diameter is defined as the twice of maximum value of ρ satisfying the condition of $I_\delta(\rho) = 1/e^2 \times I_c$, where I_c is the main-lobe intensity as shown in Fig. 4. We call δd in Eq. (7) a defocus distance.

3.2. Evaluation of the Focal Depth of Focusing Systems

To evaluate the focal depth of three focusing systems (i), (ii), and (iii), we calculated the spot diameters and maximum side-lobe intensities at each defocus distance by using Eq. (6). The calculated results are shown in Fig. 5. Figure 5(a) denotes that the system of case(ii) generates the smallest spot diameter in the area of defocus distance less than $\pm 3\mu$m. But the spot diameter of case(ii) enlarges discontinuously at the defocus distance of $\pm 3\mu$m because the first side-lobe intensity becomes more than $1/e^2$ of main-lobe.

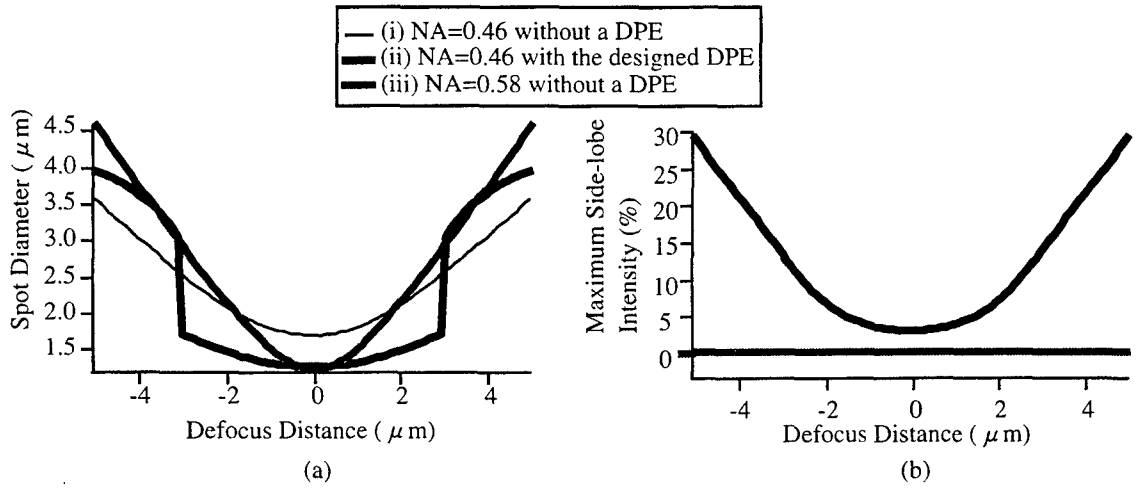

Figure 5. Changes of (a) spot diameters and (b) maximum side-lobe intensity versus defocus distance in three configurations of focusing systems.

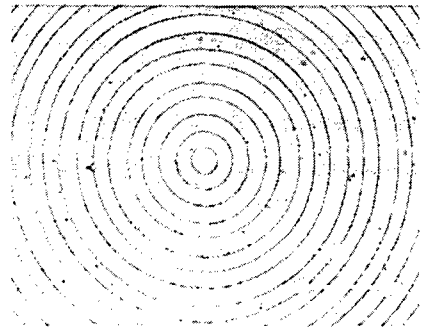

Figure 6. The microscopic picture of the fabricated DPE.

Now let us consider the case of the photoresist with 1.5μm thickness, which is a maximum thickness we usually use. When the defocus distance is 1.5μm, the spot diameter increases about 1.1 times of the focal spot size in case(ii), while 1.5 times in case(iii). On the other hand, the maximum side-lobe intensity is almost zero constantly in cases(i) and (iii), while it reaches to 4.6% of main-lobe intensity in case(ii) when the defocus distance is 1.5μm. However this side-lobe is too weak to affect pattern drawing because of nonlinear sensitivity of the photoresist material.

From above consideration, it is shown that the focusing system with the DPE has a wider focal depth with a small spot than the system without a DPE. So the focusing system with the designed DPE is useful to achieve higher resolution of pattern drawing, and more efficient than using a focusing lens with larger NA alone.

4. EXPERIMENTAL RESULTS

The designed DPE was fabricated by using a photolithography and reactive ion etching processes. In a lithography process, the laser beam lithography system developed in our laboratory and AZ1500 of photoresist (Hoechst Industry Limited) were utilized. And a compact ECR ion shower system (EIS-200ER; Elionix Inc.) was used in etching process. Figure 6 shows the microscopic picture of the fabricated DPE. The ring patterns were drawn as multiple concentric circles by changing their radii with 0.5μm pitch. The etching depth was 491nm corresponding to π phase modulation for wavelength 422nm of a He-Cd laser, which is the light source of the lithography system we use.

The fabricated DPE was mounted on the laser beam lithography system to evaluate its effectiveness. In this section, the function of the DPE is verified by measuring the spot diameters obtained in the laser beam system and

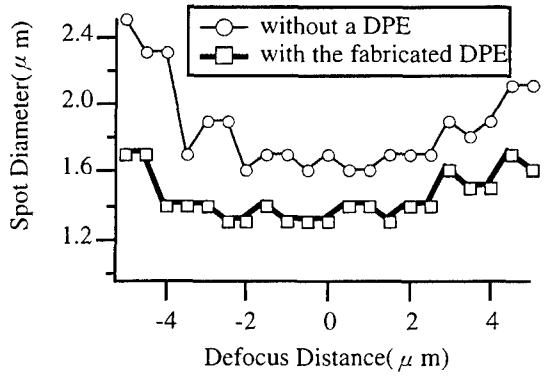

Figure 7. The measured spot diameters of the focusing system with or without the DPE.

its performance is evaluated by drawing some basic patterns.

4.1. Measurement of the Spot Diameters by Knife Edge Method

The diameters of focal and defocused spot patterns were measured by the scanning knife edge method. The scanning interval of knife edge is 0.1μm and a defocus interval was set as 0.5μm in the direction of optical axis by the control of a piezo-actuator. The positional repeatability of a x-stage used for scanning the knife edge is about 0.2μm. To reduce noise, the measured data were filtered with Savitzky-Golay filter[13] and fitted to two dimensional gaussian profile. The measured spot diameters by changing the defocus distance within $\pm$5μm are shown in Fig. 7. Although it is difficult to specify the focal plane precisely in the measured data, the minimum diameters can be estimated as 1.6μm for the system without a DPE and as 1.3μm for the system with the DPE. By this result, it is confirmed that the diameter is reduced by using the DPE. The spot diameter obtained with the DPE varies a little at the range of defocus distance from -4μm to 2μm and increases gradually at outside of this range. The case without a DPE also shows same characteristics. These results agree with the simulation results of Fig. 5(a).

4.2. Evaluation of the Resolution by Pattern Drawing

Firstly, in order to verify the effect of the side-lobes of a focal spot, the point spread patterns were drawn. Figure 8 shows the microscopic pictures of these patterns drawn on the photoresist; (a) is obtained without a DPE, and (b) with the DPE. For the comparison, we tested another DPE generating strong side-lobes, whose intensity is over 20% of main-lobe intensity. Figure 9(a) shows the calculated spot pattern by using the DPE with strong side-lobes and (b) is the picture of the obtained point spread patterns on the photoresist. The ring patterns generated by side-lobes appear around each central spot in Fig. 9. On the other hand, the effect of side-lobes is not presented in Fig. 8(b). These results demonstrate that the side-lobes produced by the DPE designed adequately do not make adverse effects on the pattern drawing. This is because that the side-lobe intensity is small enough (about 2.7% in design) and the photoresist have weak sensitivity to such small intensity.

In the next, line and space patterns were drawn on a photoresist and line width was measured. Straight lines with 3μm period were drawn by scanning laster beam. The photoresist images obtained by the scanning electronic microscopy (SEM) are shown in Fig. 10; (a) shows the pattern obtained without a DPE, and (b) shows the pattern with the DPE. It is verified from Fig. 10 that the width of drawn lines are reduced from 1.2μm in (a) to 1.0μm in (b). While the side-lobe area for each adjacent line is overlapped in Fig. 10(b), undesirable patterns do not appear. From these results, the drawing resolution is surely improved by the DPE developed by us. The reducing rate for a spot diameter was measured as about 83% in the experiment whereas the computer simulation predicted it as 74%. The reason of this difference mainly depends on the difference of threshold level for the focal spot. The line width obtained in the experiment depends on the sensitivity of the photoresist material, while the spot diameter is defined by the spot area with $1/e^2$ intensity of main-lobe in the computer simulation. The fabrication error in etching depth also affects the line width.

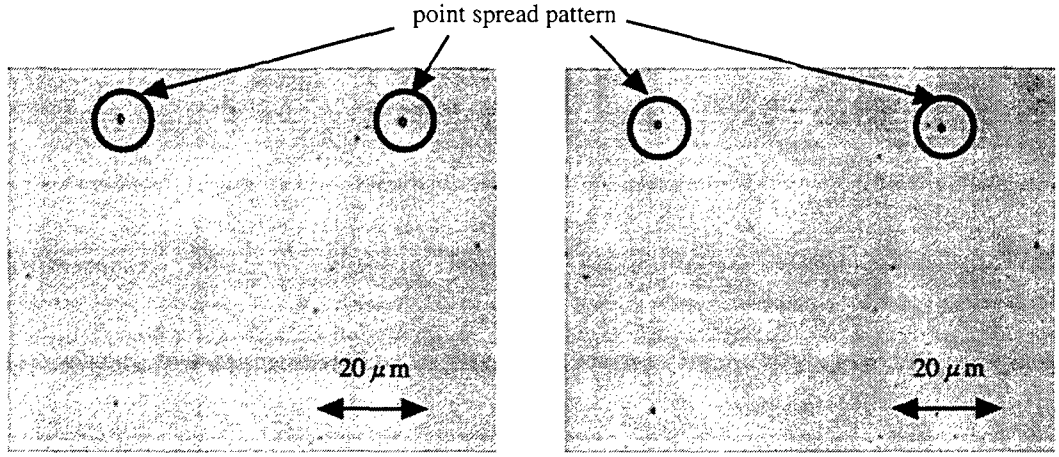

Figure 8. The microscopic pictures of point spread patterns on the photoresist material obtained (a) without a DPE and (b) with the fabricated DPE.

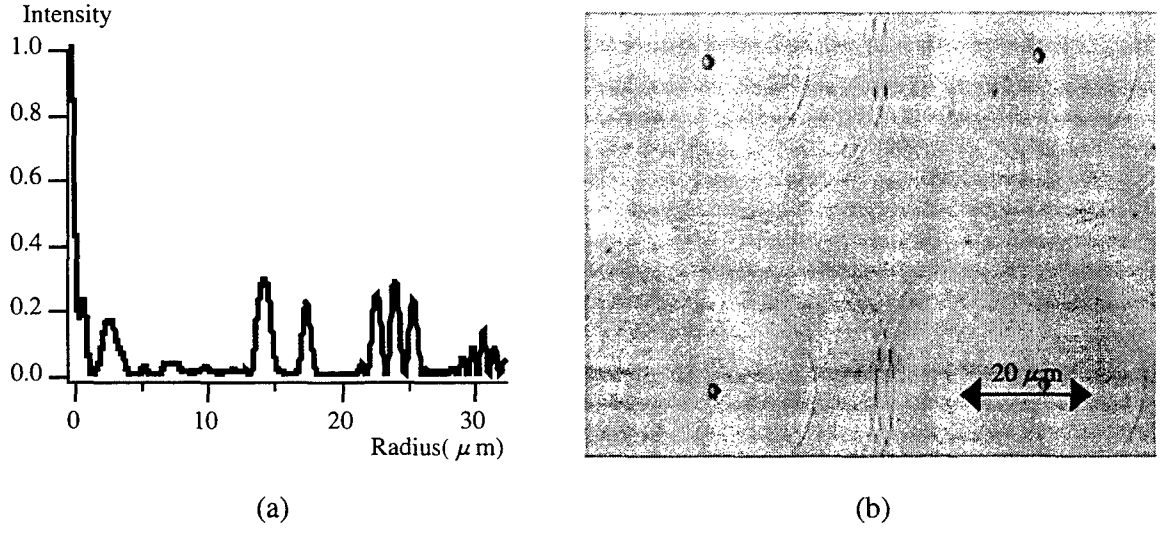

Figure 9. The experimental results for the DPE generating the strong side-lobes. (a) The calculated focal spot pattern and (b) point spread patterns drawn on a photoresist material by using the DPE.

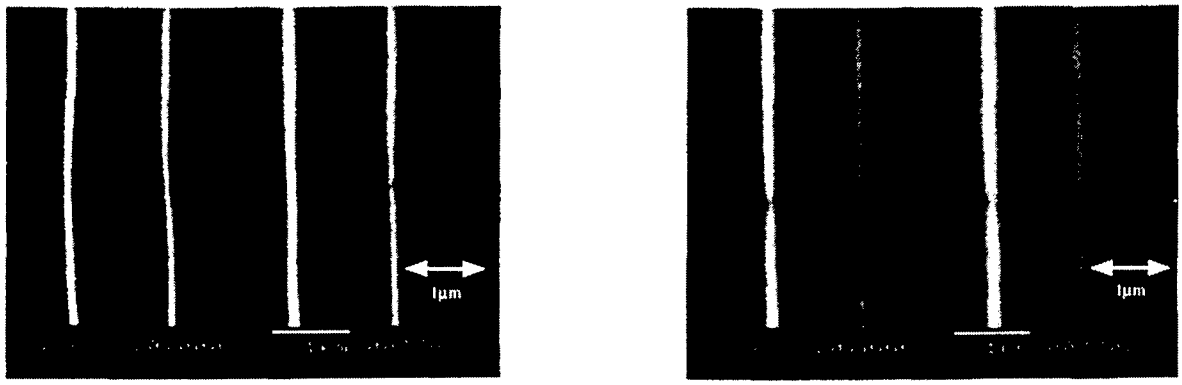

(a) without a DPE (b) with the DPE

Figure 10. SEM images of line and space patterns.

5. CONCLUSION

In this paper, we presented about the design, fabrication, and evaluation of the DPE to reduce the focal spot diameter, and to improve the resolution of the laser beam lithography system. By using iterative method with new constraints, we designed the rotation symmetrical DPE that can reduce the spot diameter to 74% in the cost of increase of side-lobe intensity to 2.7%. The DPE was fabricated by a lithography process and was mounted on the laser beam lithography system to evaluate the effectiveness of the DPE. We confirmed experimentally that the minimum line width of drawn pattern is reduced from 1.2μm to 1.0μm by using the fabricated DPE. It was also verified that the focal depth of the system with the DPE is wider than that of the system without the DPE when both systems produce the same focal spot size. Thus, it can be shown that the developed DPE is useful for a laser beam lithography process to obtain finer structures than the conventional system with a focusing lens alone. For improving the resolution of the focusing system, it is well-known to use a focusing lens with large NA or a short wavelength of light. Utilization of the DPE described in this paper is another approach and it would be expected to improve the density of an optical memory system, the resolution of a laser beam printer, or other focusing systems.

REFERENCES

1. D. Prongué, H. P. Herzig, R. Dändliker, and M. T. Gale, "Optimized kinoform structures for highly efficient fan-out elements," *Appl. Opt.* **31**, pp. 5706–5711, 1992.
2. T. Dresel, M. Beyerlein, and J. Schwider, "Design of computer-generated beam-shaping holograms by iterative finite-element mesh adaption," *Appl. Opt* **35**, pp. 6865–6874, 1996.
3. A. Vasara, J. Turunen, and A. T. Friberg, "Realization of general nondiffracting beams with computer-generated holograms," *J. Opt Soc. Am. A* **6**, pp. 1748–1754, 1989.
4. M. S. Kim and C. C. Guest, "Simulated annealing algorithm for binary phase only filters in pattern classification," *Appl. Opt.* **29**, pp. 1203–1208, 1990.
5. R. W. Gerchberg and W. O. Saxton, "A practical algorithm for the determinaion of phase from image and diffraction plane pictures," *Optik* **35**, pp. 237–246, 1972.
6. V. V. Kotlyar, I. V. Nikolski, and V. A. Soifer, "Adaptive iterative algorithm for focusators synthesis," *Optik* **88**, pp. 17–19, 1991.
7. J. Ojeda-Castañeda, L. R. Berriel-Valdos, and E. Montes, "Bessel annular apodezers: imaging characteristics," *Appl. Opt.* **26**, pp. 2770–2772, 1987.
8. J. Ojeda-Castañeda, R. Ramos, and A. Noyola-Isgleas, "High focal depth by apodization and digital restoration," *Appl. Opt.* **27**, pp. 2583–2586, 1988.
9. M. Mino and Y.Okano, "Improvement in the OTF of a defocused optical system through the use of shaded apertures," *Appl. Opt.* **10**, pp. 2219–2223, 1971.

10. F. Wyrowski, "Diffractive optical elements: iterative calculation of quantized blazed phase structures," *J. Opt. Soc Am. A* **7**, pp. 961 – 969, 1990.
11. A. E. Siegman, "Quasifast hankel transform," *Opt. Lett.* **1**, pp. 13–15, 1977.
12. V. V. Kotlyar, P. G. Seraphimovich, and V. Soifer, "An iterative weight-based method for calculating kinoforms," *Proc. SPIE Image Processing and Cmmputer Optics* **2363**, pp. 175–183, 1994.
13. A. Savitzky and M. J. E. Golay, "Smoothing and differentiation of data by simplified least squares procedures," *Anal. Chem.* **36**, pp. 1627–1639, 1964.